Marcell Villanueva, Fredy; Linshu, He; Dajun, Xu

Kick Solid Rocket Motor Multidisciplinary Design Optimization Using Genetic Algorithm

Kick Solid Rocket Motor Multidisciplinary Design Optimization Using Genetic Algorithm

Fredy Marcell Villanueva[1], He Linshu[1], Xu Dajun[1]

ABSTRACT: In this paper, a multidisciplinary design optimization (MDO) approach of a solid propellant kick rocket motor is considered. A genetic algorithm optimization method has been used. The optimized kick solid rocket motor (KSRM) is capable of delivering a small satellite of 200 kg to a circular low earth orbit (LEO) of 600 km altitude. The KSRM should accelerate from the initial apogee velocity of 5000 m/s up to the orbital insertion velocity of 7560 m/s. The KSRM design variables and the orbital insertion trajectory profile variables were optimized simultaneously, whereas the mass characteristics of the payload deployment module were assigned. A depleted shutdown condition was considered, to avoid the necessity of a thrust termination device, resulting in a reduced total mass of the KSRM. The results show that the proposed optimization approach was able to find the convergence of the optimal solution with highly acceptable value for conceptual design phase.

KEYWORDS: Kick solid rocket motor, Multidisciplinary design optimization, Genetic algorithm.

INTRODUCTION

Using small solid rocket motors (SRM) for space applications became very attractive, because of their advantages compared with liquid propellant driven rocket engines, especially for insertion of small payloads into a circular Low Earth Orbit (LEO). Simplicity, reliability, and easy to fabricate and operate, are some of the main characteristics of the SRMs. In this article, a specific design used for insertion of a payload into a specified orbit commonly known as kick solid rocket motors (KSRM) are analyzed and discussed.

Previous works were performed on analysis of several options of upper stages for different launch vehicles (LV) (McGinnis and Joyner, 2005), and in design and optimization of upper stages for transfer from LEO to geostationary earth orbit (Motlagh and Novinzadeh, 2012).

Casalino *et al.,* (2011) carried out an optimization of a hybrid upper stage configuration with a special emphasis on the grain geometry. He Linshu and Murad (2005) developed an improved method for conceptual design of multistage solid rockets based on depleted shutdown condition, which means that the SRM has to burn all-contained propellant, resulting in a reduced gross mass.

The genetic algorithm (GA) global optimization method is increasingly being used in optimization of aerospace and propulsion systems (Kamran *et al.*, 2009; Tedford and Martins, 2010; Riddle *et al.*, 2007; Rafique *et al.*, 2009). Bayley and Hartfield (2007) used

GA in multidisciplinary design optimization (MDO). Davis (2001), Goldberg (1989), and Fletcher (2000) provided a comprehensive description and step-by-step implementation of the GA in design and optimization of complex systems.

The insertion process of a payload into the orbit of a typical solid propellant LV start after a ballistic flight phase, when the upper stage is in the apogee altitude, which correspond to the required circular orbital altitude. At this point, to reach the required orbital velocity, a kick impulse is necessary, and for this purpose, a KSRM is required. Its propellant should be burnt completely (depleted shutdown condition), avoiding the use of a thrust termination device, resulting in a reduced total mass of the KSRM. The insertion accuracy is maintained by using an attitude control system grouped in a payload deployment module (PDM).
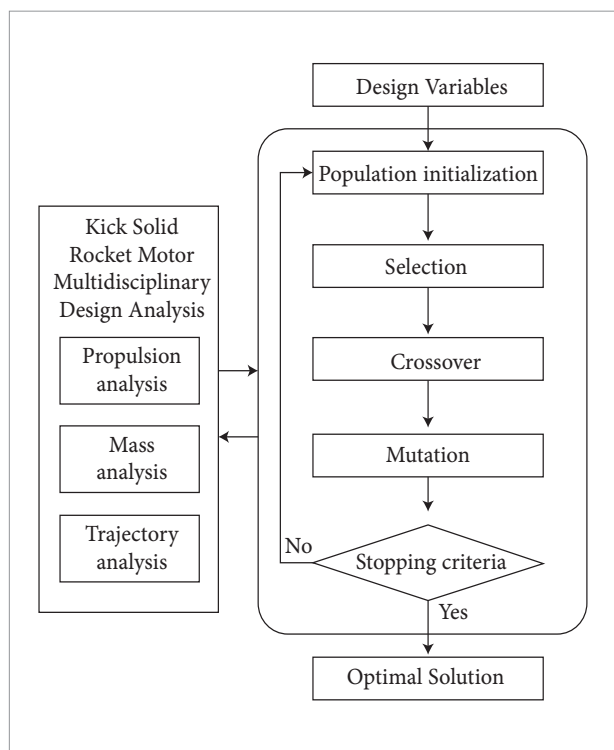
Thus, the objective of this article is to describe the optimization approach of a KSRM for insertion of a small payload into a prescribed circular LEO orbit by using a well-performed GA optimization method as a global optimizer.

Figure 1. Genetic algorithm optimization approach.

OPTIMIZATION STRATEGY

The MDO approach considered aims to find the KSRM optimal design and the corresponding trajectory to successfully accomplish the specified mission, which is an insertion of a small payload into a prescribed circular LEO orbit. To accomplish this task, a widely used GA optimization method is considered. The main advantage of this method relies on its independency of initial point to perform the optimization.

The GA is considered to be a powerful heuristic global optimization tool in solving complex optimization problems that traditionally has been solved using the approximated analysis. An additional advantage of the GA is the ability to solve discrete and continuous variables.

The operation sequence of the GA optimization method is shown in Fig. 1. Here, the procedure starts with the assignment of the design variables, the algorithm performs several operations as population initialization, selection,

crossover and mutation until the optimal solution is reached, whereas all the considered constraints are satisfied.

The drawback of the GA is its computational expense, because a large number of function evaluations are required before finding the optimal solution.

The main characteristics of the GA are presented in Table 1.

Table 1. Genetic algorithm characteristics.

Variables	Characteristics
Generations	200
Population size	100
Stopping criteria	function tolerance 10e^{-6}
Population type	double vector
Selection	stochastic uniform
Crossover	single point pc=0.8
Mutation	uniform pm=0.25641
Reproduction	elite count=2
Function evaluation	2000

KICK SOLID ROCKET MOTOR MODEL

KICK SOLID ROCKET MOTOR DEFINITION

Mission analysis

The mission is to deliver a small payload to a circular LEO orbit of h_f=600 km altitude. An upper stage composed of a KSRM, a PDM of 100 kg, and, a small payload of 200 kg is considered for this research.

The KSRM should accelerate the upper stage from an initial apogee velocity of V_0=5000 m/s up to the insertion orbital velocity of V_f=7560 m/s, whereas the PDM containing the attitude control system maintains the upper stage witting the allowable insertion accuracy.

KSRM design

There can be many variants of design options; however, for this research effort, a classical configuration was considered. The rocket motor case is considered to be made of high-strength steel, titanium alloy for attachment parts, the ignition system is located in the forward central part of the chamber, and the nozzle has a thrust vector control (TVC) system.

Grain characteristics

For the present analysis, a hydroxyl-terminated polybutadiene (HTPB) grain is selected due to its high performance and suitable for space applications. The composite grain has an internal port and an equivalent length was adopted instead of a complex 3D geometry. This assumption considerably simplifies the model and is acceptable for the conceptual design phase.

PROPULSION ANALYSIS

The propulsion analysis of the KSRM can be calculated using the classical approach. Sutton and Biblarz (2001) and He Linshu (2004a, 2004b) provided a detailed propulsion analysis including the essential parameters, like propellant mass flow rate, burn time, thrust, and nozzle parameters. In this analysis, a constant in time burning surface is considered; a grain geometry shape coefficient k_s is used to represent the constant burning surface of the grain S_b as a function of the equivalent length of grain L_{gn} and diameter D_{gn} as follows:

$$k_s = \frac{S_b}{D_{gn} L_{gn}} \tag{1}$$

The mass of the grain is calculated from the design variables and propulsion analysis, and the burn time t_b, mass of the grain m_{gn}, and mass flow rate $\dot{m}_{gn}$ of the grain are calculated as shown below:

$$m_{gn} = \frac{\pi}{4} \rho_{gn} \eta_v \lambda_{gn} D_{gn}^3 \tag{2}$$

$$t_b = \frac{\pi \eta_v D_{gn}}{4u\, k_s} \tag{3}$$

$$\dot{m}_{gn} = \rho_{gn} u\, S_b = \rho_{gn} u\, k_s \lambda_{gn} D_{gn}^{\;2} \tag{4}$$

$$\lambda_{gn} = \frac{L_{gn}}{D_{gn}} \tag{5}$$

where, u is the burning rate of propellant, ρ_{gn} is the density of grain, L_{gn}=L_m+0.3151D_m is the equivalent length of the grain, D_{gn}=D_m is diameter of the grain, L_m is the rocket motor cylindrical length, λ_{gn} is fineness ratio of the grain (grain length/diameter), and η_v is the grain volumetric loading fraction.

The nozzle throat area A_t, expansion ratio ε, and nozzle exit area A_e are calculated as follows:

$$A_t = \frac{\rho_{gn} u\, S_b}{\Gamma_0\, p_{c\max}} \sqrt{R_c T_c} \tag{6}$$

$$\varepsilon = \frac{\Gamma_0}{\left(\dfrac{p_e}{p_c}\right)^{\frac{1}{\gamma}} \sqrt{\dfrac{2\gamma}{\gamma-1}\left[1-\left(\dfrac{p_e}{p_c}\right)^{\frac{\gamma-1}{\gamma}}\right]}} \tag{7}$$

$$A_e = A_t \varepsilon \tag{8}$$

$$\Gamma_0 = \sqrt{\gamma}\left(\frac{2}{\gamma+1}\right)^{\frac{\gamma+1}{2(\gamma-1)}} \tag{9}$$

where, S_b is the burning surface of grain, R_c=326 $J/(kg.K)$ is gas constant, T_c=2790K^o is temperature in the combustion chamber, p_e is exit pressure, p_c is chamber pressure,

$p_{cmax}=1.1p_c$ is the maximum value of chamber pressure, and $\gamma=1.21$ the specific heat ratio of the gas.

The vacuum specific impulse I_{sp}^{vac}, and the thrust T can be calculated as shown below:

$$I_{sp}^{vac}=I_{sp}^a+\left(\frac{p_e}{p_c}\right)^{\frac{\gamma-1}{\gamma}}\frac{R_c\,T_c}{g^2\,I_{sp}^a} \tag{10}$$

$$T=I_{sp}^{vac}\dot{m}_{gn}-p_a A_e \tag{11}$$

where, p_a is the atmospheric pressure, I_{sp}^a is average specific impulse, g is acceleration due to gravity, $\dot{m}_{gn}$ is mass flow, and A_e is the nozzle exit area.

MASS ANALYSIS

The mass of the upper stage is represented by the following equations:

$$m_0=m_{KSRM}+m_{PDM}+m_{PAY} \tag{12}$$

$$m_{KSRM}=m_{st}+\dot{m}_{gn} \tag{13}$$

where, m_0 is the upper stage mass, m_{KSRM} is kick solid rocket mass, m_{PDM} is payload deployment module mass, m_{PAY} is payload mass, and m_{st} is the structural mass of the KSRM.

He Linshu (2004b) provided a detailed calculation of the KSRM structural mass, which is highly acceptable for conceptual design phase, and is shown in the following equation:

$$\begin{aligned}m_{st}=&\,m_{cy}+m_{c1}+m_{c2}+m_q+m_{j1}+m_{j2}\\&+m_{in,c1}+m_{in,c2}+m_{in,cy}+m_{noz,ec}+m_{noz,sh}\\&+m_{noz,in}+m_{ig}+m_{TVC}+m_{cab}+m_{ap}\end{aligned} \tag{14}$$

It is composed of the mass of the motor cylinder, m_{cy}, motor dome ends, m_{c1} and m_{c2}, forward and aft skirts, m_q, forward and aft joints, m_{j1} and m_{j2}, forward and aft insulation liners, $m_{in,c1}$ and $m_{in,c2}$, cylindrical section insulation liner, $m_{in,cy}$, nozzle expansion cone, $m_{noz,ez}$, nozzle spherical head, $m_{noz,sh}$, nozzle insulation, $m_{noz,in}$, igniter, m_{ig}, thrust vector control, m_{TVC}, cables, m_{cab}, and mass of attachment parts, m_{ap}.

The materials selected for the motor case are high-strength steel and titanium alloy, ethylene propylene diene monomer for chamber insulation, and carbon phenolic for the nozzle, whereas the factor of safety was taken as 1.5.

The mass of cylindrical part of the chamber can be calculated by the following relation:

$$m_{cy}=\frac{3K_{cy}\pi\,f\,f_p D_{ch}^3 p_c\lambda_{gn}}{8\sigma_b} \tag{15}$$

where, $K_{cy}=1.02$ is the ratio of the case cylindrical length to rocket motor equivalent length (L_{cy}/L_m), which was obtained from statistics, f is factor of safety, $D_{ch}=D_m$ is diameter of chamber, and σ_b is the ultimate strength of the chamber material.

The mass of the forward motor dome end m_{c1} can be calculated as follows:

$$m_{c1}=\frac{\pi\lambda_e^2 D_{ch}^3 f\,f_p\,p_c}{8(\lambda_e^2-1)\sigma\cos\theta_2}\left[1-\frac{1}{1+(\lambda_e^2-1)\sin^2\theta_2}\right] \tag{16}$$

where, $\lambda_e=2$ is the chamber ellipsoid ratio, σ is strength ratio $\sigma=\sigma_b/\rho_{cl}$, where, ρ_{cl} is the density of closure material and θ_2 taken as 60°.

The relative pressure in the chamber f_p is determined as shown below:

$$f_p=\frac{p_{c,max}}{p_c} \tag{17}$$

The aft motor dome end is calculated as follows:

$$\begin{aligned}m_{c2}=&\,\frac{\pi\lambda_e^2 D_{ch}^3 f\,f_p p_c}{8(\lambda_e^2-1)\sigma\cos\theta_2}\\&\cdot\left[\frac{\lambda_e^2 D_{ch}^2-(\lambda_e^2-1)d_n^2}{\lambda_e^2 D_{ch}^2}-\frac{1}{1+(\lambda_e^2-1)\sin^2\theta_2}\right]\end{aligned} \tag{18}$$

where, $d_n=0.4D_{ch}$ is the diameter of closure rear end opening for nozzle.

The mass of the forward and aft skirts of the SRM are calculated as follows:

$$m_q=\pi D_{ch}^2\rho_q\delta_q\frac{l_{q1}+l_{q2}}{D_{ch}} \tag{19}$$

where, ρ_q is the density of skirt material, δ_q is thickness of skirts, and l_{q1} and l_{q2} are lengths of forward and aft skirts.

The mass of the forward joint to the igniter m_{j1} and the aft joint to nozzle assembly m_{j2} can be calculated as shown below:

$$m_{j1}=\frac{3\pi\,f\,f_p p_c d_n^3}{\sigma_j} \tag{20}$$

$$\sigma_j = \frac{\sigma_{bj}}{\rho_j} \tag{21}$$

$$m_{j2} = m_{j1} \tag{22}$$

where, σ_j is the strain of joint, ρ_j is density of the joint material, and σ_{bj} is ultimate strain of joint.

The forward and aft insulation liners $m_{in,c1}$, $m_{in,c2}$ and cylindrical section insulation liner $m_{in,cy}$ can be determined using Eqs. 23 to 25.

$$m_{in,c1} = \frac{1}{4}\rho_{in}\pi D_{ch}^2 R_a t_b \tag{23}$$

$$m_{in,c2} = \frac{\rho_{in}\pi D_{ch}^2 R_a t_b}{4(\lambda_e^2 - 1)}\left[\frac{\lambda_e^2 D_{ch}^2 - (\lambda_e^2 - 1)d_n^2}{D_{ch}^2}\right] \tag{24}$$

where, ρ_{in} is the density of insulation material and R_a is the rate of ablation of the insulation material.

$$m_{in,cy} = \pi D_{ch} L_{cy}\rho_{in}\frac{(\varepsilon_{in}c_{in}\rho_{in} + \alpha_{gi}c_{cy}\rho_{cy}\delta_{cy})}{\alpha_{gi}c_{in}\rho_{in}}$$
$$\cdot\left[\sqrt{1 - \frac{2\varepsilon_{in}(\ln\theta_p c_{cy}\rho_{cy}\delta_{cy} + \alpha_{gi}t_b)\alpha_{gi}c_{in}\rho_{in}}{\ln\theta_p(\varepsilon_{in}c_{in}\rho_{in} + \alpha_{gi}c_{cy}\rho_{cy}\delta_{cy})^2}} - 1\right] \tag{25}$$

$$\theta_p = \frac{T_g - T_{cy}}{T_g - T_I} \tag{26}$$

where, L_{cy} is the length of case cylindrical section, ε_{in} is heat transfer coefficient of insulation material, c_{in} is specific heat capacity of insulation, c_{cy} is specific heat capacity of the cylindrical section, α_{gi} is heat transfer coefficient from gas to insulation, ρ_{cy} is density of the case cylindrical section material, T_g is temperature of gas, T_{cy} is allowable temperature of the cylindrical section, and T_I is the initial temperature of the cylindrical section.

The mass of the nozzle expansion cone $m_{noz,ec}$, nozzle spherical head $m_{noz,sh}$, and nozzle insulation $m_{noz,in}$ are expressed using the Eqs. (27), (28), and (29), respectively.

$$m_{noz,ec} = \rho_{ec}\frac{\pi}{4\sin\beta_n}\left(\frac{A_e}{A_t} - 1\right)d_t$$
$$\cdot\left[f\times 0.67\sqrt[6]{\frac{d_e}{d_t} - 1}\,(1-S)^{\frac{4}{3}}\sqrt{\frac{P_{cmax}\sigma_{ec}}{E_{ec}}}\right] \tag{27}$$

where, ρ_{ec} is the material density of the expansion cone, β_n is nozzle expansion half angle, S is submerged coefficient of the nozzle, d_e is the nozzle exit diameter, d_t is diameter of throat, σ_{ec} is ultimate strength of the expansion cone material, and E_{ec} is the elastic modulus of expansion cone material.

$$m_{noz,sh} = 3.656\,\rho_{sh}d_t^3 \tag{28}$$

where, ρ_{sh} is the material density of spherical head of nozzle.

$$m_{noz,in} = \rho_{innz}S_{nz}\delta_{innz} \tag{29}$$

where, ρ_{innz} is the material density of the nozzle insulation, S_{nz} is surface area of the nozzle, and δ_{innz} is the thickness of the nozzle insulation.

The igniter mass m_{ig}, can be calculated as follows:

$$m_{ig} = 1.454\left(\frac{7\pi d_t^2}{4}\right)^{1.2} \tag{30}$$

The nozzle thrust vector control mass m_{TVC}, is considered as shown below:

$$m_{TVC} = 0.235m_{noz} \tag{31}$$

The mass of the cables m_{cab} and attachment parts m_{ap} are expressed in Eqs. (32) and (33).

$$m_{cab} = 1.3L_{cy}\,\rho_c \tag{32}$$

where, ρ_c is the linear density of the cable (kg/m).

And finally, the mass of the attachment parts is calculated as follows:

$$m_{ap} = (6.13\cdot 10^{-7})D_m^2 L_{cy}^{1.148} \tag{33}$$

TRAJECTORY ANALYSIS

For trajectory analysis, a 3 degree of freedom (3DOF) model has been developed and implemented using SIMULINK (Zipfel, 2007; Fleeman, 2001). This model uses the upper stage mass, including the KSRM, PDM and payload mass, and thrust as input parameters. The upper stage is considered as a point-mass in two-

dimensional coordinate systems (2D) over a spherical and non-rotating earth, where the Coriolis and centrifugal forces are not considered.

The considered state variables are velocity, flight path angle, altitude, and mass, whereas the control variable is the programmed angle of attack. The trajectory analysis computes the state variables by solving the equation of motion presented in Eq. 34, and evaluating the constraint conditions at every phase of flight.

Figure 2 illustrates the forces acting on the upper stage and below a set of governing equations of motion (He Linshu, 2004a; Xiao, 2001).

$$
\begin{aligned}
\frac{dV}{dt} &= \frac{T\cos\alpha}{m} - g\sin\vartheta \\
\frac{d\vartheta}{dt} &= \frac{T\sin\alpha}{mV} - \frac{g\cos\vartheta}{V} + \frac{V}{R_e + h}\cos\vartheta \\
\frac{dh}{dt} &= V\sin\vartheta \\
\frac{dl}{dt} &= \frac{R_e}{R_e + h}V\cos\vartheta \\
\alpha &= \eta + \varphi - \vartheta \\
\eta &= \frac{l}{R_e}
\end{aligned}
\tag{34}
$$

where, V is the velocity, m is vehicle mass, φ is pitch angle, θ is trajectory angle, ϑ is flight path angle, η is range angle, R_e is radius of earth, h is height above the ground, and l is the range.
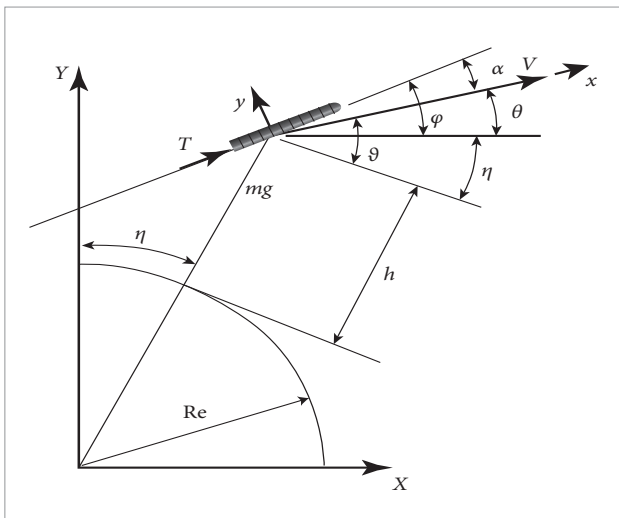
Figure 2. Forces acting on the upper stage.

The axial and normal overload coefficients can be calculated in a body centered velocity coordinate systems (0, x, y) and represented as follows:

$$
n_x = \frac{T\cos\alpha}{mg} \le n_{x\max}
\tag{35}
$$

$$
n_y = \frac{T\sin\alpha}{mg} \le n_{y\max}
\tag{36}
$$

The density variation with altitude can be represented as follows:

$$
\rho = \rho_0\, e^{(-h/\beta)}
\tag{37}
$$

The variation of gravity with altitude can be represented as follows:

$$
g = \frac{\mu}{(R_e + h)^2}
\tag{38}
$$

where, ρ_0 is the sea level density, β is the density scale height, and μ is the earth gravitational parameter.

The required circular orbital insertion velocity V_f for a given final altitude h_f can be represented as follows:

$$
V_f = \sqrt{\frac{\mu}{h_f + R_e}}
\tag{39}
$$

ORBIT INSERTION PROFILE SEQUENCE

The trajectory optimization was performed considering different constraints that prevent the KSRM, its components, and the payload from failure. The trajectory is modeled considering a depleted shutdown condition at the time of insertion, as follows (He Linshu, 2004b; Qazi and He Linshu, 2005):

Initial Condition

For a typical solid propellant LV orbital payload insertion, the trajectory starts from the time where the upper stage is in the apogee altitude of h_0=600 km, the initial condition is that the flight path angle should be ϑ_0=0 degrees, and the initial velocity V_0=5000 m/s, the angle of attack also should be zero degrees α_0=0.

Pitch over insertion maneuver

After ignition, the upper stage accelerates by the power of the KSRM and flies following the orbital altitude. This phase

comprises up to the end of burning time (depleted shutdown condition). A second order curve is fitted from the initial time to the final insertion time; this curve represents the programmed angle for this phase.

Insertion condition

At this time all parameters should comply with the insertion accuracy requirements. The flight path angle at this time should approach zero degrees and within the boundary conditions, $\vartheta_f \approx 0$, the programmed angle of attack is constrained to approach zero $\alpha_f \approx 0$, the orbital velocity should be $V_f = 7560$ m/s corresponding to $h_f = 600$ km altitude, and the normal and axial acceleration should be less than its allowable maximum values.

ORBIT INSERTION PROFILE FORMULATION

The variation of the flight path angle during insertion flight has substantial influence on the injection accuracy in orbit, acceleration loads, and final orbital velocity. It is influenced by a programmed angle of attack. Figure 3 explains the insertion maneuver, and the angle of attack is programmed using the following relations (He Linshu, 2004a; He Linshu, 2004b; Xiao, 2001):

$$\alpha_{prog}(t) = \alpha_{max}\sin^2 f(t) \tag{40}$$

$$f(t) = \frac{\pi(t - t_1)}{k_m(t_2 - t) + (t - t_1)} \tag{41}$$

$$k_m = \frac{t_m - t_1}{t_2 - t_m} \tag{42}$$

where, α_{max} is the maximum angle of attack, $\alpha_{prog}(t)$ is the programmed angle of attack, k_m is the insertion maneuver variable, t is time of flight, t_m is time corresponding to maximum angle of attack, t_1 is time of start of insertion maneuver, and t_2 is insertion time, coincident in value with the KSRM burning time t_b.

DESIGN OPTIMIZATION PROBLEM

OBJECTIVE FUNCTION

For the present research effort, the objective is to minimize the KSRM mass m_{KSRM}. The mathematical description of the objective function is as follows:
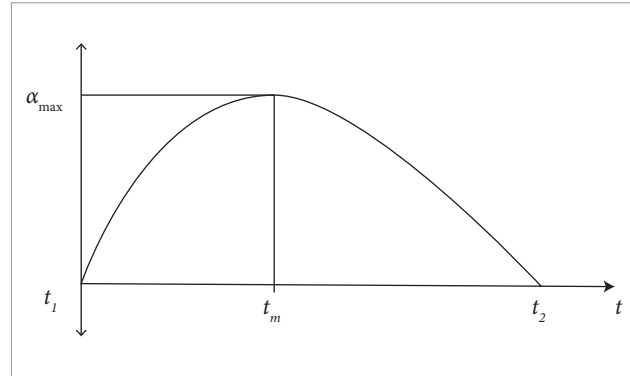
Figure 3. Programmed angle of attack variation.

$$\min m_{KSRM} = f(X) \tag{43}$$

$$g_j(X) \le 0 \tag{44}$$

$$h_k(X) = 0 \tag{45}$$

$$X_{lb} \le X_i \le X_{ub} \tag{46}$$

where, X is the set of variables, X_{lb} is lower bound of variables and X_{ub} is the upper bound of variables.

DESIGN VARIABLES

The variables considered in the KSRM design and the insertion maneuver trajectory can be represented in Eq. (47) and listed in Table 2.

$$X = [L_m, D_m, p_c, p_e, k_s, u, \rho_{gn}, \eta_v, \alpha_{max}, k_m] \tag{47}$$

Table 2. Design variables.

	Variables	Symbol	Units
X1	Rocket motor cylindrical length	L_m	m
X2	Rocket motor diameter	D_m	m
X3	Chamber pressure	p_c	Pa
X4	Nozzle exit pressure	p_e	Pa
X5	Coefficient of grain shape	k_s	
X6	Grain burning rate	u	m/s
X7	Grain density	p_{gn}	kg/m3
X8	Grain volumetric loading	η_v	
X9	Maximum angle of attack	α_{max}	deg
X10	Insertion maneuver variable	k_m	

DESIGN CONSTRAINTS

To prevent the failure of the upper stage, KSRM and PDM, several constraints were selected, and are listed in Table 3.

DESIGN SEQUENCE

This section describes a step-by-step sequence for multidisciplinary design of the KSRM as follows:

Step	Procedure	Reference
1	Define initial variables X	Eq. 47
2	Define constraints C	Table 3
3	Calculate grain mass $\dot{m}_{gn}$	Eq. 2
4	Calculate burning time t_b	Eq. 3
5	Calculate mass flow $\dot{m}_{gn}$	Eq. 4
6	Calculate throat area A_t	Eqs. 6 – 9
7	Calculate specific impulse I_{sp}^{vac}	Eq. 10
8	Calculate thrust T	Eq. 11
9	Calculate KSRM mass m_{KSRM}	Eqs. 13 – 33
10	Set constant values m_{PDM}, m_{PAY}	Mission
11	Calculate upper stage mass m_0	Eq. 12
12	Trajectory conditions $V_0, h_0, \vartheta_0, \alpha_0$	Orbit Insertion Profile Sequence
13	Calculate $\alpha_{prog}(t)$	Eqs. 40 – 42
14	Calculate $\rho(h)$	Eq. 37
15	Calculate $g(h)$	Eq. 38
16	Calculate $V(t), \vartheta(t), h(t), l(t),$	Eq. 34
17	Calculate overloads n_x, n_y	Eqs. 35, 36
18	Calculate final values V_f, h_f, ϑ_f	Eq. 34
19	Check constraints	Table 3
20	Back to step 1	

OPTIMIZATION RESULT

The optimization results show that the optimized KSRM as well as the upper stage insertion trajectory

Table 3. Design constraints.

	Constraints	Value	Units
C1	Orbit insertion velocity	$V_f=7560\pm1$	m/s
C2	Final altitude	$h_f=600\pm0.1$	km
C3	Axial overload	$n_x \leq 12$	
C4	Normal overload	$n_y \leq 2$	
C5	Maximum angle of attack	$\alpha_{max} \leq 10$	deg
C6	Orbit insertion angle	$\vartheta_f=0\pm0.02$	deg
C7	Fineness grain ratio	$\lambda_{gn} \leq 2$	
C8	Nozzle exit diameter	$d_e \leq 0.95\, D_m$	m
C9	KSRM total length (including nozzle)	$L_{KSRM} \leq 1.8$	m
C10	Burning time	$t_b \leq 50$	s
C11	Nozzle expansion ratio	$\varepsilon \leq 80$	

profile successfully reached the objective function. The optimized values of design variables were obtained, and these variables did not violate the considered design constraints. Table 4 shows the lower bound, upper bound, and optimized values of the design variables.

There are several parameters that characterize the KSRM; however, only the most important were calculated from the optimized design variables and are presented in Table 5.

Table 4. Optimum values of variables.

Variables		Lower Bound	Upper Bound	Optimized Value
L_m	m	0.65	0.90	0.8141
D_m	m	0.65	0.90	0.8140
p_c	Pa	60e5	70e5	65.901e5
p_e	Pa	0.05e5	0.20e5	0.0581e5
k_s		1.50	1.90	1.5050
u	m/s	6.5e-3	8.5e-3	6.651e-3
ρ_{gn}	kg/m³	1725	1735	1727.01
η_v		0.80	0.86	0.8176
α_{max}	deg	7.5	9.0	8.3601
k_m		0.28	0.45	0.3222

Table 5. KSRM optimum values.

| Parameter	Symbol	Unit	Optimized Value
Upper stage mass	m_0	kg	1061.81
Rocket motor mass	m_{KSRM}	kg	761.816
Grain mass	m_{gn}	kg	679.358
Structural mass	m_{st}	kg	82.488
Burning time	t_b	s	45.677
Specific impulse[vac]	I_{sp}^{vac}	N.s/kg	2544.12
KSRM total length	L_{KSRM}	m	1.733
Nozzle throat diameter	d_t	m	0.062
Nozzle exit diameter	d_e	m	0.5409
Nozzle expansion ratio	ε		76.13

Figures 4 and 5 illustrate the optimized insertion trajectory profile of the upper stage. From Fig. 4 it can be seen that the burning time of the KSRM is 45.67 seconds, the end of burning time shows coincidence with the required insertion parameters. Additionally, the figures evidenced that the payload is inserted at the required altitude of 600 km and the obtained circular orbital velocity is 7560 m/s. The insertion flight path angle is within the required accuracy, whereas the axial and normal overloads were maintained within the constraints limits.
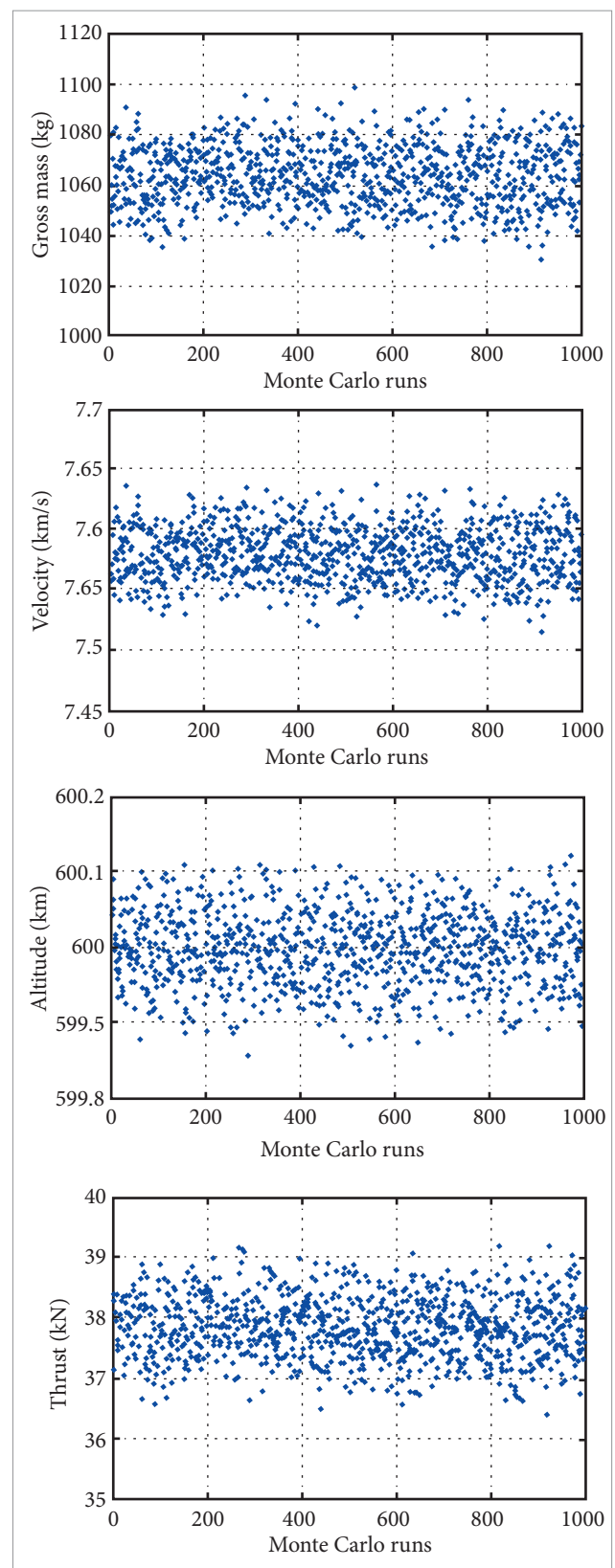
SENSITIVITY ANALYSIS

Monte Carlo analysis is widely used in system and early stage of design. It provides a relatively accurate statistical evaluation of the response distribution under input uncertainties. Monte Carlo sensitivity analyses of the main KSRM parameters were conducted to investigate the effect of uncertainties of design variables over the expected result. For this analysis, a ±1% error was added to every optimized value of design variables. The results are presented in Table 6, and the scatter plot is shown in Fig. 6.

The GA optimization method considered successfully reached the optimal solution, a population of 100 with 200 generation was sufficient to perform the present study; however, several trials had been carried out to obtain the desired accuracy of the optimal solution.
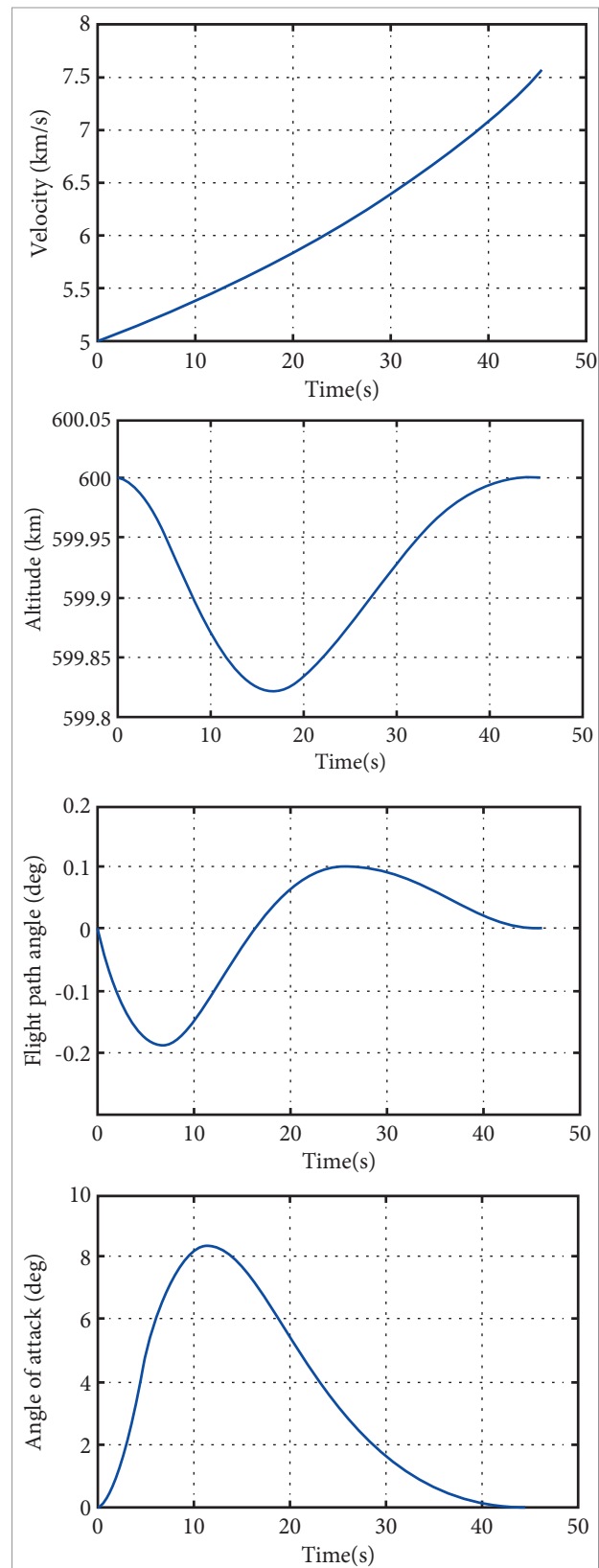
Figure 4. Insertion trajectory profile of the upper stage.
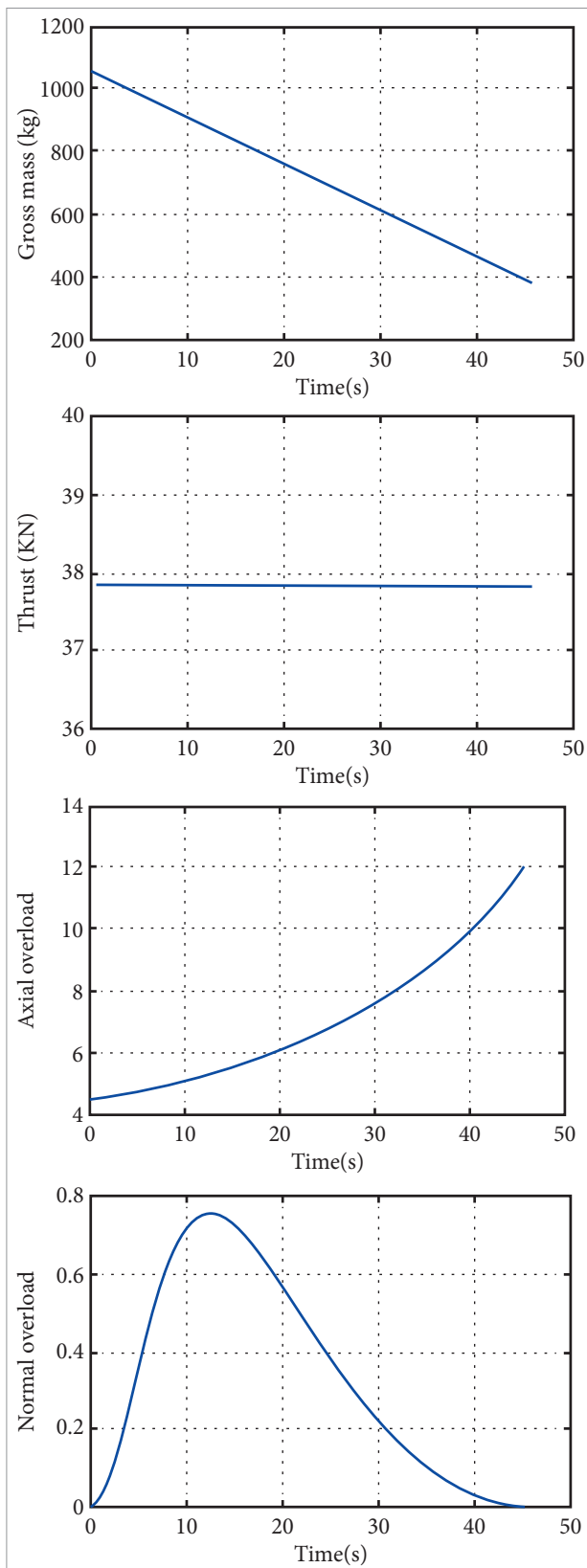
Figure 5. Flight parameters of the upper stage.

Figure 6. Monte Carlo sensitivity analysis.

Table 6. Monte Carlo results.

Parameter	Unit	Minimum value	Maximum value	Mean value	Standard deviation
Gross mass	kg	1030.6	1098.2	1063.9	11.771
Velocity	m/s	7515.1	7648.2	7579.2	0.0219
Altitude	km	599.86	600.12	600.00	0.0473
Thrust	kN	36.383	39.184	37.846	0.497

CONCLUSION

A GA based optimization approach has been applied to conceptual design and optimization of a KSRM. The advantage of the GA relied on its independency of initial point to calculate the optimum. A 2D dynamic model was developed to simulate the orbital insertion trajectory of the upper stage composed of the PDM of 100 kg, the optimized a payload of 200 kg. A sensitivity analysis was conducted using Monte Carlo method to investigate the variation of the main parameters of the KSRM. The emphasis of this research was to find the optimal KSRM design and the upper stage insertion trajectory profile characteristics required for insertion a small payload into a circular LEO orbit of 600 km.

The results of the KSRM parameters are shown in Tables 4 and 5 and its insertion trajectory profile is shown in Figs. 4 and 5, and Monte Carlo sensitivity analysis shown in Fig. 6 evidenced the validity of the used approach for the early stage of the design process.

ACKNOWLEDGMENTS

REFERENCES

Anderson M.B., Burkhalter, J. and Jenkins, R., 2001, "Multi-Disciplinary Intelligent Systems Approach to Solid Rocket Motor Design. Part I: Single and Dual Goal Optimization", 37th AIAA/ASME/SAE/ASEE Joint Propulsion Conference and Exhibit, AIAA, paper 2001-3599.

Bayley, D.J. and Hartfield, R.J., 2007, "Design Optimization of a Space Launch Vehicles for Minimum Cost using a Genetic Algorithm", AIAA 43rd AIAA/ASME/SAE/ASEE Joint Propulsion Conference and Exhibit, AIAA, paper 2007-5852.

Casalino, L., Pastrone, D. and Simeoni, F., 2011, "Hybrid Rocket Upper Stage Optimization: Effects of Grain Geometry", AIAA 47th AIAA/ASME/SAE/ASEE Joint Propulsion Conference and Exhibit, AIAA, paper 2011-6024.

Davis, L., 2001, "The Handbook of Genetic Algorithm", Van Nostrand Reingold, New York.

Fleeman, L.E., 2001, "Tactical, Missile Design", AIAA, Reston.

Fletcher, R., 2000, "Practical Methods of Optimization", John Wiley & Sons.

Goldberg, D., 1989, "Genetic Algorithm in Search, Optimization and Machine Learning", first edition, Addison-Wesley–Longman Publishing Co., Reading, MA.

He Linshu, 2004a, "Launch Vehicle Design", Beijing University of Aeronautics and Astronautics Press, Beijing.

He Linshu, 2004b, "Solid Ballistic Missile Design", Beijing University of Aeronautics and Astronautics Press, Beijing.

He Linshu and Murad Y., 2005, "An Improved Method for Conceptual Design of Multistage Solid Rockets based on Depleted Shutdown", Journal of Solid Rocket Technology, Vol. 28, No 2, paper 120-125.

Kamran, A., Lian, G., Godil, J., Siddique, Z., Zeeshan, Q. and Rafique, A., 2009, "Design and Performance Optimization of Finocyl Grain", AIAA Modeling and Simulation Technologies Conference 10-13 August 2009, Chicago, Illinois, AIAA, paper 2009-6234.

McGinnis, P.M. and Joyner, C.R., 2005, "Upper Stage Propulsion Options for Various Launch Vehicle Architectures", AIAA 41st AIAA/ASME/SAE/ASEE Joint Propulsion Conference and Exhibit, AIAA, paper 2005-4180.

Motlagh, J.A. and Novinzadeh, A.B., 2012, "Solid Upper Stage Design Process using Finite Burn Maneuvers for Low Earth Orbit–Geosynchronous Earth Orbit Transfer Phase", Institution of Mechanical Engineers, Part G: Journal of Aerospace Engineering.

Qazi, M. and He Linshu, 2005, "Rapid Trajectory Optimization using Computational Intelligence for Guidance and Conceptual Design of Multistage Space Launch Vehicles", AIAA Guidance, Navigation, and Control Conference and Exhibit, AIAA, paper 2005-6062.

Rafique, A.F., He Linshu, Zeeshan, Q., Kamran, A., Nisar, K. and Wang, X.W., 2009, "Integrated System Design of Air Launched Small Space Launch Vehicle using Genetic Algorithm", 45th AIAA/ASME/SAE/ASEE Joint Propulsion Conference and Exhibit, AIAA, paper 2009-5506.

Riddle, D.B., Hartfield, R.J., Burkhalter, J.E. and Jenkins, R., 2007, "Genetic Algorithm Optimization of Liquid Propellant Missile Systems", AIAA Aerospace Sciences Meeting and Exhibit, AIAA, paper 2007-0362.

Sutton, G.P. and Biblarz, O., 2001, "Rocket Propulsion Elements", Wiley-Interscience, New York.

Tedford, N.P. and Martins, J.R., 2010, "Benchmarking Multidisciplinary Design Optimization Algorithms", Optimization and Engineering, Vol. 11, No 1, paper 159-183.

Xiao, Y.I., 2001, "Rocket Ballistics and Dynamics", Beijing University of Aeronautics and Astronautics.

Zipfel, P.H., 2007, "Modeling and Simulation of Aerospace Vehicle Dynamics", second edition, AIAA Education Series, AIAA, Reston.